

This article was published in an Elsevier journal. The attached copy is furnished to the author for non-commercial research and education use, including for instruction at the author's institution, sharing with colleagues and providing to institution administration.

Other uses, including reproduction and distribution, or selling or licensing copies, or posting to personal, institutional or third party websites are prohibited.

In most cases authors are permitted to post their version of the article (e.g. in Word or Tex form) to their personal website or institutional repository. Authors requiring further information regarding Elsevier's archiving and manuscript policies are encouraged to visit:

<http://www.elsevier.com/copyright>



Surface and structural disorder in MBE and sputtering deposited Cu thin films revealed by X-ray measurements

M. Salvato^{b,c,*}, A. Aurigemma^{a,c}, A. Tesaro^{a,c}, C. Attanasio^{a,c}

^a*Dipartimento di Fisica “E.R. Caianiello”, Università degli Studi di Salerno, Via S. Allende I-84081, Baronissi, SA, Italy*

^b*Dipartimento di Fisica, Università degli Studi di Roma “Tor Vergata”, Via della Ricerca Scientifica, I-00193 Roma, Italy*

^c*Laboratorio Regionale “SuperMat” CNR-INFN, Via S. Allende I-84081, Baronissi, SA, Italy*

Received 17 April 2007; received in revised form 18 July 2007; accepted 23 July 2007

Abstract

Copper thin films have been deposited on Si substrates by molecular beam epitaxy (MBE) at different deposition rates varying from 1 up to 22 Å/s. X-ray reflectivity and θ – 2θ measurements have shown that the surface roughness correlation length, the structural disorder and the grain dimensions are strongly affected by the deposition rate. Comparing these results with those obtained for sputtered deposited thin films with a low deposition rate (2.5 Å/s), a clear similarity between the MBE samples deposited with the highest deposition rate and the sputtering Cu films is observed. This result has been interpreted considering the different energies of the particles that approach the substrate in the two deposition techniques.

© 2007 Elsevier Ltd. All rights reserved.

Keywords: Molecular beam epitaxy (MBE); X-ray reflectivity; X-ray diffraction; Reflection high energy electron diffraction (RHEED)

1. Introduction

A renewed interest in Cu thin films deposited with different techniques has been recently observed [1–11] because of the possibility of employing this material for interconnections, cap layers or contacts in the microelectronic industry. Due to the low cost, Cu is replacing Al in the fabrication of electronic devices. Because the electronic industry is projected towards nanoscale applications, the possibility of obtaining very thin films with flat surfaces plays a fundamental role in the project of new electronic components. Cu thin films can be obtained with different methods. Sputtering [1–5], electroplating [6–9] and thermal evaporation [10,11] are the most commonly used deposition techniques even though the structural and electrical quality of the films strongly depend on the deposition process. In particular, if one is interested in the purity of the final product, thermal evaporation in ultra-high

vacuum conditions should be used. Moreover, in order to avoid interdiffusion between different layers of the same device, which in the most common cases is a multilayered structure of different elements, the Cu deposition should be performed at low or at room substrate temperature. This gives rise to textured rather than epitaxial growth confirming that a control of grain dimensions and surface roughness is of fundamental importance when fabricating layered structures [2,3,7,10]. Because the deposition time is one of the decisive parameters in the electronic industry, a study of the surface quality of Cu thin films on Si substrates deposited at different rates can give additional indications about the best growth technique to adopt.

2. Experimental details

We deposited Cu thin films on Si(100) substrates by molecular beam epitaxy (MBE) using a 6 kW electron gun. All the samples have been obtained in the same evaporation conditions except for the deposition rate. The starting pressure was 1×10^{-10} Torr and the pressure during the deposition was 2×10^{-8} Torr. Because our study is directed towards the fabrication of multi-layer-based devices,

*Corresponding author. Dipartimento di Fisica, Università degli Studi di Roma “Tor Vergata”, Via della Ricerca Scientifica, I-00193 Roma, Italy. Tel.: +39 06 72594506; fax: +39 06 2023507.

E-mail address: matteo.salvato@roma2.infn.it (M. Salvato).

where any annealing procedure which causes interdiffusion between the layers and photoresist damage should be avoided, no substrate heating process was applied and the studied samples had been obtained at room substrate temperature. The final nominal thickness was 300 Å for all the samples. Cu thin films with the same thickness were deposited by magnetron sputtering using an Ar pressure of 1×10^{-3} mbar. The base pressure in the chamber was 2×10^{-7} Torr. As in the case of MBE, the substrate was at room temperature during the sputtering deposition. In both the systems, the deposition rates were controlled by using a quartz crystal oscillator thickness monitor which was previously calibrated by depositing test Cu thin films and measuring their thickness by X-ray reflectivity measurements. The results reported here are concerned with three different MBE films deposited with rates of 1, 4 and 20 Å/s and a sputtering-deposited sample with a rate of 2.5 Å/s which are representative of more than 100 samples deposited with the same techniques.

The surfaces of the MBE thin films were monitored during the growth by reflection high energy electron diffraction (RHEED). All the samples were analyzed by X-rays after the deposition using a Philips X-Pert MRD diffractometer and performing both high- and low-angle measurements with Cu $K_{\alpha 1}$ radiation ($\lambda = 1.54056$ Å) obtained by filtering the primary beam with a four crystal Ge(220) asymmetric monochromator and a graded parabolic mirror. For the high-angle measurements, a 1/16° slit were positioned between the sample and the detector, while a parallel beam collimator was used for low-angle measurements reducing the diffracted beam divergence to 0.01°. The high-angle spectra were both θ – 2θ and pole figure measurements were made in order to determine the orientation of the samples. On the other hand, low-angle reflectivity measurements were performed in order to detect the specular reflectivity intensity and the diffuse part of the scattered rays (rocking curves). The scan reflectivity data were collected and shown, for all the samples, in reflectivity maps which contain both the information on the specular and on the diffuse reflectivity spectra.

3. Experimental results and discussion

The diffraction patterns obtained by RHEED analysis during the deposition of the MBE samples showed the presence of rings already from the first deposited atomic layers. In Fig. 1a, a typical RHEED pattern obtained for an MBE-deposited thin film is shown. The presence of diffracted rings rather than streaks or spots as in the case of epitaxial films, indicates that, independent of the deposition rate, the surface of the samples is not oriented and that no in-plane epitaxial relation exists between the substrate and the films. This is confirmed by texture measurements performed on all the samples and is shown in Fig. 1b for the (110) reflection of an MBE grown sample. The figure shows the presence of a diffuse spectrum at about 33° in the form of a ring which is characteristic of the in-plane

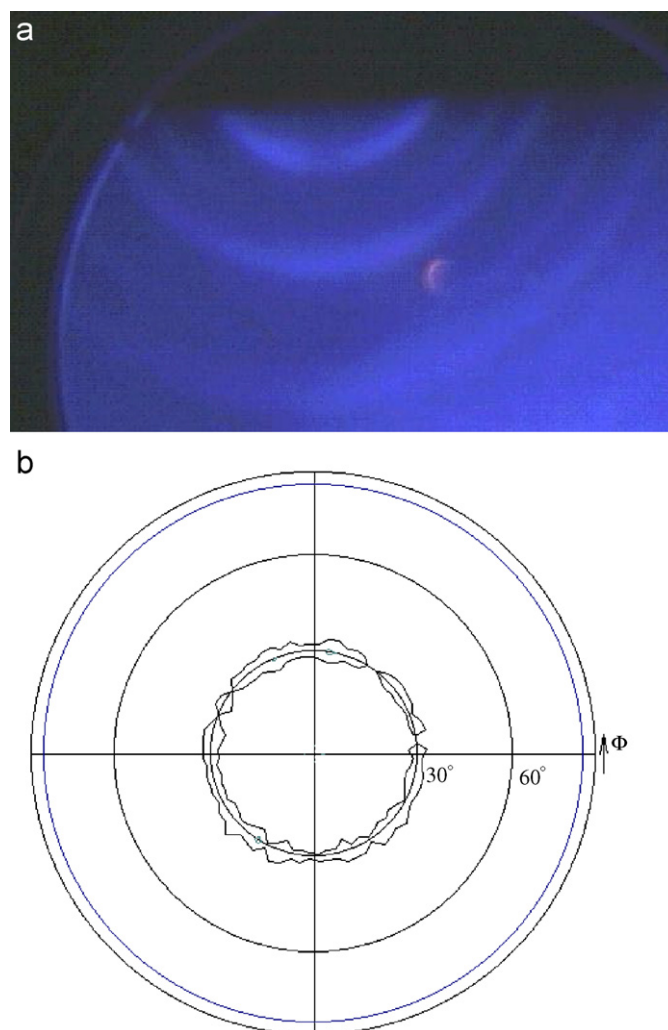


Fig. 1. (a) Typical RHEED pattern and (b) pole figure for Cu thin films deposited by MBE.

textured growth with the (111) planes parallel to the substrate surface. Moreover, the absence of single reflections spaced $\Delta\Phi = 120^\circ$ in place of, or superimposed on, the observed diffuse spectrum excludes any interpretation about the possibility of an in-plane epitaxial growth. Although RHEED analysis was not performed in the case of sputtering-deposited films, X-ray pole figure and θ – 2θ measurements showed the same textured growth of these films. In Fig. 2a–d, the Cu(111) θ – 2θ peaks for the three MBE and for the sputtering-deposited samples are shown. The position of the peaks gives a (111) lattice spacing $d_{(111)} = 2.05$ Å for both the MBE and the sputtering-deposited samples, which corresponds to a lattice parameter of 3.55 Å for the Cu cubic lattice unit cell. The lowest peaks in Fig. 2a–c, on the left side of the Cu(111) reflections, are due to the presence of CuO in the Cu films and they are observable only in the samples deposited by MBE. The intensity of these peaks decreases as the deposition rate increases indicating that, in the case of MBE, oxygen atoms are easily incorporated in the lattice structure during slow deposition processes. The presence of

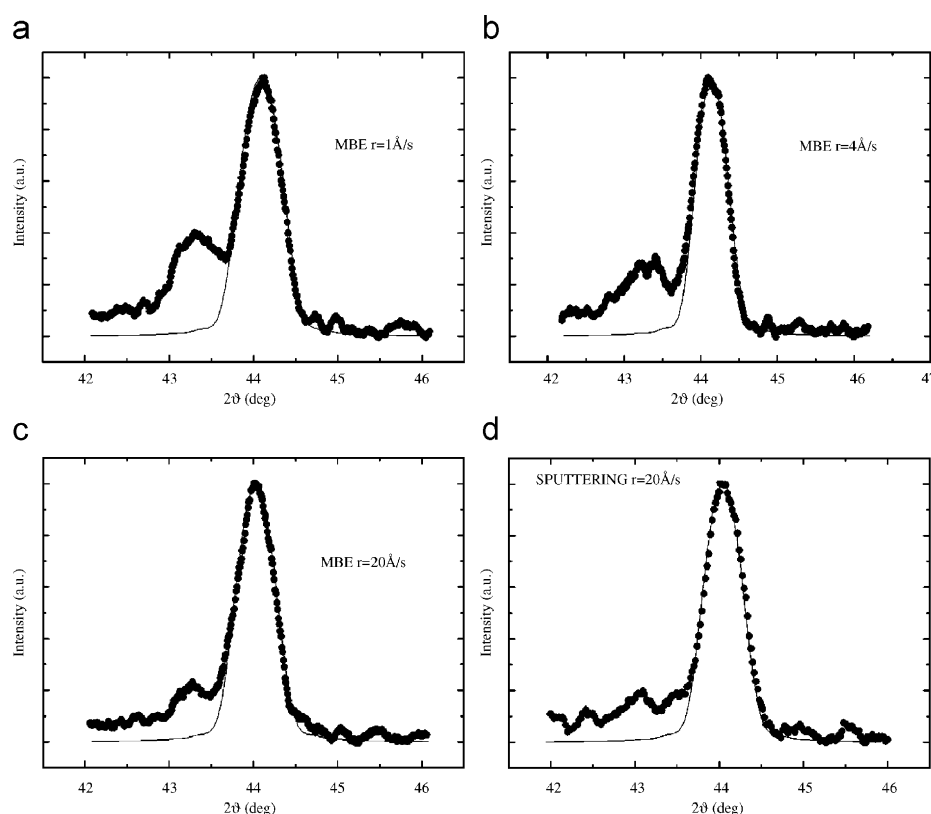


Fig. 2. Cu(111) Bragg peaks for MBE deposited thin films with rates of (a) 1 Å/s, (b) 4 Å/s, (c) 22 Å/s and (d) sputtering deposited thin film with rate 2.5 Å/s. The lines are fits of the data obtained using a Gaussian distribution of the crystalline structure (see the text for details).

oxide inside the MBE samples is difficult to explain if one consider the low evaporation pressure which corresponds to a mean free path of about 104m for the oxygen molecules. Nevertheless, the absence of CuO in the sputtering-deposited samples suggests that most of the oxide is formed during the migration of the evaporated ions from the electron gun crucible to the substrate in the MBE vacuum chamber or on the substrate surface due to the ionic nature of the evaporated species. Both these processes are strongly favored with respect to the sputtering where the target to substrate distance is about 100 times shorter and molecule aggregates rather than ionic species are deposited.

The experimental data of Fig. 2 were fitted using a refinement procedure to simulate the Cu structure [12] introducing a Gaussian disorder between the crystalline planes. The lines in Fig. 2 were obtained using the variance of the Gaussian distribution of the Cu lattice spacing around the average lattice distance $d_{(111)} = 2.05 \text{ Å}$ as fitting parameter and using the least square method for the normalized intensities [12]. The fitting procedure allowed to estimate the (111) grain's dimensions and the average structural disorder, whose values are shown in Table 1. The errors associated to structural disorder, the grains dimension and the roughness correlation length were determined taking into account the spreading associated to the experimental data. For all the θ - 2θ measurements we have $\Delta 2\theta = 0.005$ on the 2θ angle and $\Delta I/I_0 = 10^{-3}$ for the

normalized intensity I/I_0 . In the case of the MBE samples, an increase of the grain dimensions and a decrease of the structural disorder are observed when the deposition rate is increased. Comparing these values with those obtained in the case of the sputtered Cu film, it appears that the structural properties of the sputtered sample are similar to that observed in the case of the MBE thin film deposited with the highest deposition rate.

Fig. 3a–d shows the reflectivity maps obtained for the three MBE and the sputtering-deposited films. The maps are represented in a dimensional reciprocal space units where Q_{\perp} and Q_{\parallel} are the longitudinal and the transverse directions, respectively, with magnitude $\lambda/2D$ where D is the layer thickness. All the maps consist of a specular and a diffuse component [13]. The specular component of the reflectivity spectrum is obtained fixing the $Q_{\parallel} = 0$ position and moving along Q_{\perp} (perpendicular to the sample surface). The diffuse component is obtained moving along the Q_{\parallel} direction at a constant value of Q_{\perp} (parallel to the sample surface). The specular part of the spectra are also reported in the insets where the presence of a critical angle (at $Q_{\perp} \cong 70$) and of periodic Kiessig fringes, whose position and amplitude are related to the sample thickness and the surface roughness, respectively [14], are clearly shown.

Comparing the reflectivity maps of the MBE samples, a progressive broadening of the specular peak along the Q_{\parallel} direction is observed before the critical angle with the increase in the deposition rate. Because the specular

Table 1
Parameters of the investigated samples

Sample	Rate (Å/s)	Grains dimension (Å)	Structural disorder (Å)	Roughness correlation length (Å)
MBE1	1	186 ± 3	0.027(4)	281 ± 5
MBE2	4	200 ± 3	0.025(2)	249 ± 5
MBE3	22	226 ± 4	0.022(1)	95 ± 2
Sputtering	2.5	220 ± 4	0.020(1)	98 ± 2

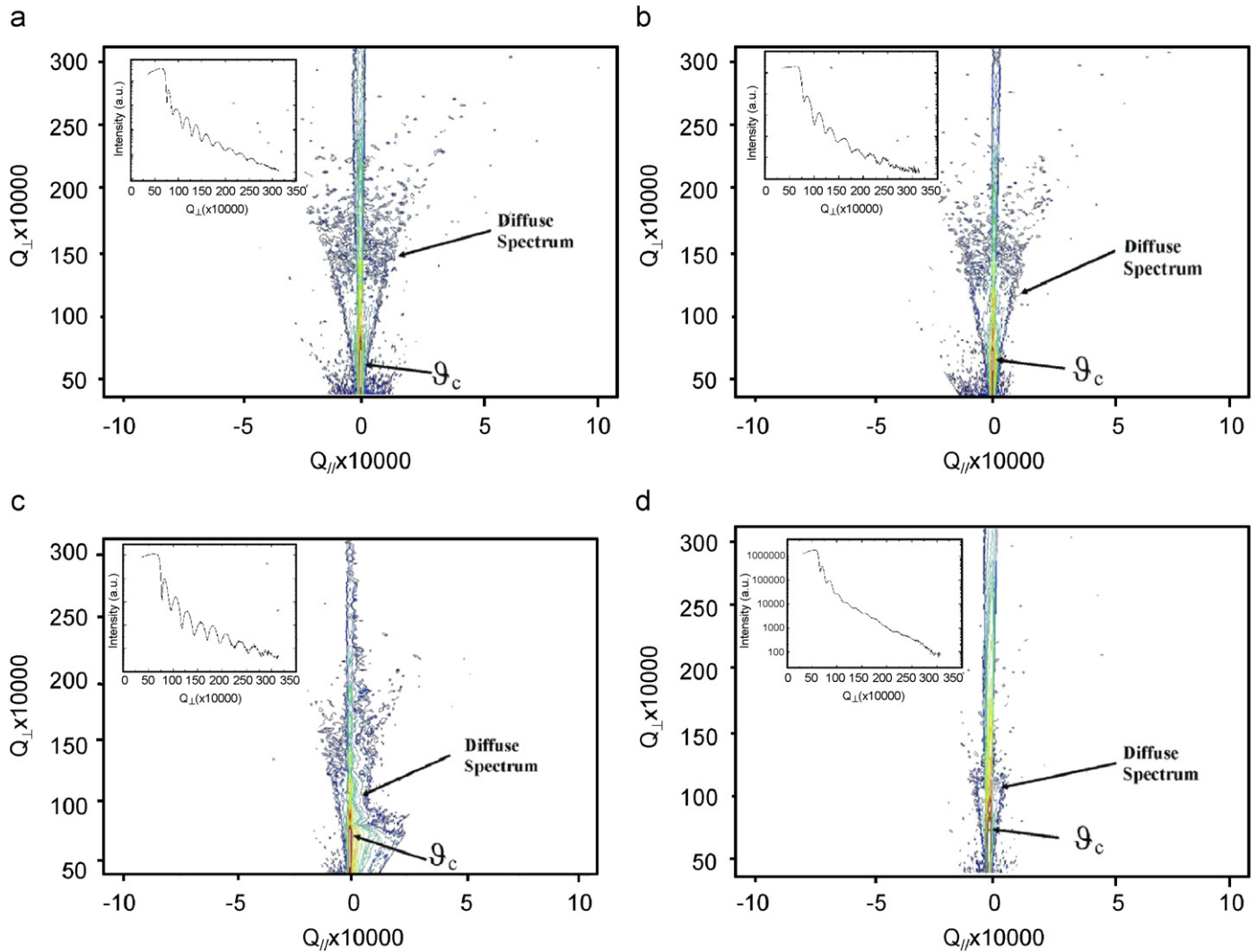


Fig. 3. Reciprocal space reflectivity maps for Cu thin films deposited by MBE (a–c) and by sputtering (d) showing the specular and the diffuse (indicated by arrows) part of the spectrum. The presence of diffuse spectrum indicates the presence of correlated roughness. θ_c is the critical angle. *Insets*: specular parts of the reflectivity spectra measured keeping $Q_{\parallel} = 0$.

intensity before the critical angle only gives indications on the quality of the surface, this effect is probably due to an increase of the surface disorder whose origin will be discussed below. Here we emphasize the presence of high asymmetric scattering which is particularly evident in the case of the highest deposition rate (Fig. 3c) and it is probably related to the formation of terraces on the film surface in the direction different from Q_{\perp} . A progressive change in the diffuse part of the spectrum is also observed for the different samples in the region of the maps next to

the specular reflection. In particular, the intensity of the diffuse part of the spectrum is higher for the samples deposited with the low evaporation rate and it is reduced in the case of the MBE sample deposited with the highest deposition rate. The almost complete absence of the diffuse part of the spectrum is also observed in the sputtering-deposited film.

The presence of the diffuse intensity is due to the presence of correlated roughness in the direction perpendicular to the sample surface [15–17]. This is commonly

observed in the case of multilayers [18,20], where the roughness can propagate periodically along the growth direction reinforcing the diffuse intensity in correspondence of the Bragg reflections. In the case of single layers, the presence of correlated roughness between the substrate and the film surface gives rise to the observed weak increase of the diffuse intensity [19,21]. The lateral correlation length of the roughness can be estimated by measuring the width of the diffuse part of the spectrum along Q_{\parallel} [19]. The values obtained for the different samples, by measuring the FWHM of the diffuse part of the spectrum in correspondence of the first Kiessig fringe [21], are reported in Table 1. For the MBE deposited thin films, the lateral correlation length decreases with the deposition rate and the minimum value approaches that obtained in the case of sputtered deposited thin films.

The experimental results clearly show a dependence of the structural and surface properties of the MBE films on the deposition rate. The formation of small and disordered grains in the structure of the copper thin films seems to be favored by a low deposition rate where smooth surfaces with long roughness correlation lengths are obtained. Moreover, increasing the deposition rate, the structural and surface features evolve towards that obtained in the case of sputtering-deposited thin films. This can be interpreted considering the different energy of the particles that impinge the substrate in the two deposition processes.

In the case of thermal evaporation, increasing the evaporation rate the supersaturation ratio increases and the lateral diffusion length of the adatoms decreases [22]. This reflects in a short lateral correlation length at high rates because the atoms are chemisorbed soon after they hit the surface. The low migration time, enhanced by the fact that the substrate is not heated, favors the formation of small oriented grains rather than the formation of flat terraces giving rise to the (1 1 1) oriented grain structure of Cu films [10]. The higher is the number of atoms that hit the surface, the lower is the time spent in a particular area of the substrate and the higher is the grain dimension. This happens because the incoming atoms are trapped in the chemical potential created by the atoms of the surface before they can escape and migrate on the surface. Therefore, a high deposition rate prevents the diffusion of the atoms from the coalescence zone where the surface energy favors the oriented grain formation.

In the case of sputtered thin films, the energy of the sputtered Cu atoms is typically about 10 times the energy of Cu atoms thermally evaporated in vacuum at the temperature of about 1000 °C [23]. For this reason the incoming Cu atoms are soon chemisorbed by the impinging surface resulting in a short diffusion length also at low deposition rates. The factor of 10 between the energy of the incoming particles in the two different deposition processes gives the reason for the similarity between the results obtained in the case of the sputtered

thin film deposited at 2.5 Å/s and the MBE thin film deposited at 20 Å/s.

4. Conclusions

X-ray analysis of Cu thin films deposited by MBE showed that both the structural and the surface properties strongly depend on the deposition rate. Increasing the deposition rate, more structurally ordered films are obtained whereas the correlation of the roughness between the substrate and the film surface is reduced. Comparing the experimental results with those obtained for a sputtered thin film, a similarity between the properties of the MBE thin film deposited with the highest rate and that shown in the case of sputtering is observed. This result is interpreted on the basis of the different energies of the particles in the two deposition processes. The possibility of obtaining sputtered high quality thin films with a high deposition rate could enable us to reduce the deposition time and the costs in the fabrication of electronic devices.

References

- [1] Detavernier C, Deduytsche D, Van Meirhaeghe RL, De Baerdemaeker J, Dauwe C. Appl Phys Lett 2003;82:1863.
- [2] Huang H, Wei HL, Woo CH, Zhang XX. Appl Phys Lett 2003;82:4265.
- [3] Wei HL, Huang H, Woo CH, Zheng RK, Wen GH, Zhang XX. Appl Phys Lett 2002;80:2290.
- [4] Huang H, Wei HL, Woo CH, Zhang XX. Appl Phys Lett 2002;81:4359.
- [5] Hau-Riege CS, Thompson CV. Appl Phys Lett 2001;78:3451.
- [6] Hau-Riege SP, Thompson CV. Appl Phys Lett 2000;76:309.
- [7] Lingg C, Gross ME, Brown WL. Appl Phys Lett 1999;74:682.
- [8] Lu L, Tao NR, Wang LB, Ding BZ, Lu K. J Appl Phys 2001;89:6408.
- [9] Seah CH, Mridha S, Chan LH. J Vac Sci Technol B 1999;17:2352.
- [10] Botez CE, Miceli PF, Stephens PW. Phys Rev B 2002;66:195413.
- [11] Botez CE, Li K, Lu ED, Elliot C, Miceli PF, Conrad EH, et al. Appl Phys Lett 2002;81:4718.
- [12] Fullerton EE, Schuller I, Vanderstraeten H, Bruynserade Y. Phys Rev B 1992;45:9292.
- [13] Holy V, Baumbach T. Phys Rev B 1994;49:10668.
- [14] Chason E, Mayer TM. Crit Rev Solid State Mater Sci 1997;22:1–67.
- [15] Sinha SK, Sirota EB, Garoff S, Stanley HB. Phys Rev B 1988;38:2297.
- [16] Holy V, Kubena J, Ohlidal I, Lischka K, Plotz W. Phys Rev B 1993;47:15896.
- [17] Phang YH, Kariotis R, Savage DE, Lagally MG. J Appl Phys 1992;72:4627.
- [18] Savage DE, Kleiner J, Schimke N, Phang YH, Jankowski T, Jacobs J, et al. J Appl Phys 1991;69:1411.
- [19] Savage DE, Schimke N, Phang YH, Lagally MG. J Appl Phys 1992;71:3283.
- [20] Fullerton Eric E, Pearson J, Sowers CH, Bader SD, Wu XZ, Sinha SK. Phys Rev B 1993;48:17432.
- [21] Gibaud A, Cowley RA, Mc Morrow DF, Ward RCC, Wells MR. Phys Rev B 1993;48:14463.
- [22] Burton WK, Cabrera N, Frank FC. Phil Trans R Soc Lond 1951;243:299; Wordenweber R. Supercond Sci Technol 1999;12:R.86.
- [23] Maissel LI, Glang R. Handbook of thin film technology. McGraw-Hill Book Company; 1970.